Desalination and Water Treatment
www.deswater.com

doi: 10.1080/19443994.2013.821044

52 (2014) 6756–6769
October

Taylor & Francis
Taylor & Francis Group

Biosorption of toxic acidic dye–Acid Blue 25, by aquatic plants

Masoud Kousha[a], Ehsan Daneshvar[a,*], Ali Reza Esmaeili[a], Hamid Zilouei[b], Keikhosro Karimi[b]

[a]*Department of Fisheries, Faculty of Natural Resources, Isfahan University of Technology, Isfahan 84156, Iran*
Tel. +98 917 8391732; email: ehsandaneshvar_iut@yahoo.com
[b]*Department of Chemical Engineering, Isfahan University of Technology, Isfahan 84156, Iran*

Received 26 April 2013; Accepted 13 June 2013

ABSTRACT

The adsorption of Acid Blue 25 (AB25) ions by aquatic plants, *Potamogeton pusillus* and *Ceratophylum demersum* from aqueous solutions was studied. The adsorption was studied as a function of solution pH (2–11), contact time (0–60 min), biomasses dosage (0.1–2.5 g/L), initial dye concentration (30–100 mg AB25 /L), biosorbents particle size (53–500 μm), addition of neutral salts (20–100 mg KNO_3/L and 20–100 mg KH_2PO_4/L), and salinity (0.5–40 g NaCl/L). The results of equilibrium adsorption were successfully described through Freundlich and Temkin isotherm for both of the biosorbents. Maximum adsorption capacity of 183.46 and 129.68 mg/g were observed for *P. pusillus* and *C. demersum*, respectively. Different kinetic models including pseudo-first order, pseudo-second order, and intra-particle diffusion were examined, and the pseudo-second order was shown to be the best model to fit the adsorption kinetics data. Thermodynamic parameters demonstrated that adsorption of AB25 ions was spontaneous and endothermic at a temperature range of 10–40°C. FTIR analysis confirmed the responsibility of several functional groups on the surface of the biosorbents for the adsorption of AB25 in this process.

Keywords: Biosorption; Aquatic plants; Acid Blue 25 dye; *Potamogeton pusillus*; *Ceratophylum demersum*

1. Introduction

Synthetic dyes are widely used in industries such as the textile, rubber, paper, plastic, leather, cosmetic, pharmaceuticals, and food ones [1]. The increasing use of dyes in various industrial applications has resulted in the discharge of toxic dye effluents into the water streams causing serious environmental pollution [2]. Dye-containing effluents are highly problematic wastewater because they affect esthetic merit and reduce light penetration, and photosynthesis. In addition, most dyes are toxic, carcinogenic, and mutagenic for humans and other organisms [3]. Wastewaters from textile and dyestuff industries are among the most difficult wastewaters for treatment because of the availability of non-oxidizable dye contents [4]. Anthraquinonic dyes, such as Acid Blue 25, represent the second most important class of commercial dyes after azo-compounds. They are an important class of commercial dyes that are primarily used for wool, polyamide, and leather dying [5]. Therefore, a suitable and effective treatment method should be devised.

*Corresponding author.

Different physical and chemical processes include ozonation, photo-oxidation, electro-coagulation, adsorption (using activated carbon), froth flotation, reverse osmosis, ion exchange, membrane filtration, and flocculation have been used for the treatment of wastewater containing dyes [6–8]. However, major disadvantages of these methods include production of toxic sludge, high operational cost, technical limitations, usually dependent on the concentration of the waste, lack of effective color reduction and sensitivity to a variable wastewater input as reported by many researchers [9].

There is a growing interest in developing low-cost and highly efficient alternative technologies for wastewater treatment. In recent years, investigations have shown that the biosorption could be an effective process for dye removal from dye wastewaters. Biologically originated materials such as barley husk [10]: cotton waste, rice milling waste [11]; hen feather [12–14]; rice husk [15]; *Corynebacterium glutamicum* [16]; decrystallized chitosan [17]; *Cosmarium* sp. [18]; *Caulerpa scalpelliformis* [19]; and aquatic plants [20,21] have been used as biosorbents to remove dyes from wastewaters. Among these materials, several biosorbents showed extraordinary properties as biosorbents. Therefore, biosorption is an ideal alternative for the decontamination of dye-containing effluents, especially for the treatment of low-concentration effluents.

In this work, aquatic plants, *Potamogeton pusillus and Ceratophylum demersum* were used in order to decolorize the dye solution containing Acid Blue 25 dye. They are commonly found in ponds, lakes, ditches, and quiet streams with moderate to high nutrient levels. They can float free in the water column and sometimes form dense mats just below the surface. They are cosmopolitan plants which can spread rapidly and grow in a wide range of aquatic habitats [22]. Therefore, the aim of the present work was to investigate the bisorption of AB25, using *P. pusillus* and *C. demersum* under experimental conditions. Thus, the influence of several operating parameters such as initial solution pH, biomass dosage, contact time, biosorbents particle size, initial dye concentration, addition of neutral salts and water salinity was examined during the adsorption of AB25 dye onto the biosorbents.

2. Materials and methods

2.1. Adsorbate

Acid Blue 25 [1-amino-9,10-dihydro-9,10-dioxo-4-(phenylamino)-2-anthracenesulfonic acid, monosodium salt] was provided from Alvan Sabet company, Iran (Fig. 1). An accurately weighed quantity of the dye was dissolved in deionized water to prepare a stock solution (1,000 mg/L). The solutions for all tests were prepared from the stock solution to the desired concentrations through successive dilutions using deionized water.

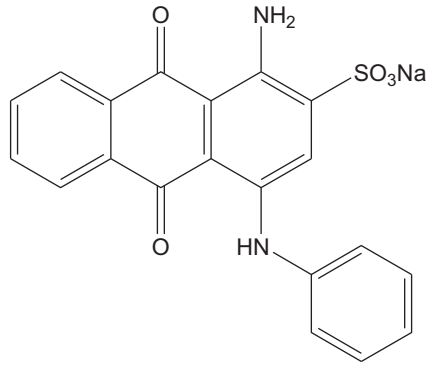

Fig. 1. Chemical structure of Acid Blue 25.

2.2. Biosorbents

The freshwater macrophytes (*C. demersum*, *P. pusillus*) were collected from Zayandeh Rood river in Isfahan province, Iran, and washed with tap and distilled water three times in order to remove other macrophytes species, adhering algae, and insect larvae. The biomasses were sun-dried for three days and then dried in an oven at 70 °C for 24 h. The dried biomasses were cut, ground in a mortar, and subsequently sieved; and the particles with a different size of 53–500 μm were used for adsorption experiments.

2.3. Adsorption experiments

Biosorption experiments were conducted in 100 mL Erlenmeyer flasks with total reaction volume of 50 mL. The pH of solution was adjusted at desired values by adding 0.1 M NaOH or HCl using pH meter (Metrohm, 620, Switzerland). Then, conical flasks were shaken for the required time period in 25 ± 2 °C on a rotary shaker (Labcon, FSIM-SPO16, USA) at 130 rpm.

To determine the optimum conditions of biosorption (with maximum AB25 decolorization), experiments were performed with varying initial solution pH (2–11), reaction time (0–60 min), biomass dosage (0.1–2.5 g/L), initial dye concentration (30–100 mg/L), biosorbent particle size (53–500 μm), nitrate and phosphate salts (20–100 mg/L), and salinity (0.5–40 g/L). All experiments were performed in duplicate and the results expressed as means values.

2.4. Biosorption isotherms

Equilibrium experiments were carried out by taking 0.4 g/L of biosorbents in 100 mL conical flasks containing 50 mL of the AB25 solution in the initial concentration range of 10–50 mg/L at initial solution pH 2. The mixture was shaken in a rotary shaker (labcon, FSIM-SPO16, United States) at 130 rpm keeping temperature constant (25 ± 2˚C). After 1 h, samples were filtered and analyzed quantitatively. Then, most commonly adsorption isotherms were applied via the Langmuir, Freundlich, Doubinin–Radushkevich (D–R) and Temkin models.

2.5. Biosorption kinetics

Biosorption kinetics of experiments was carried out in 500 mL conical flasks containing 250 mL of the dye solutions using 0.4 g/L of biosorbents at initial pH 2. The flasks were agitated for 60 min on a rotary shaker at 130 rpm under a constant temperature (25 ± 2˚C). The samples were taken at predetermined time intervals, filtered and analyzed to determine the residual dye concentrations. Three kinetic models, viz., pseudo-first-order, pseudo-second-order, and intraparticle diffusion models were employed to understand the sorption kinetics.

2.6. Thermodynamic study

Biosorption of Acid Blue 25 was finally investigated at different temperatures (10, 25, and 40˚C) in a rotary shaker under pre-optimized conditions, specifically 0.4 g/L biomasses level, 30 mg/L initial dye concentration, pH 2 and 130 rpm. Various thermodynamic parameters such as enthalpy changes (ΔH°), entropy changes (ΔS°), and Gibbs free energy changes (ΔG°) were applied to determine the nature of adsorption process.

2.7. Fourier transform infrared spectra study

FT-IR analyses within the range of 400–4,000 cm^{-1} were recorded with a Jasco-680 (Japan) spectrometer. Biosorption process was performed with 100 mL solution containing 30 mg AB25/L, initial pH 2 and 0.4 g/L of two aquatic plants. At the reaction times of 0 min (control) and 60 min, samples were taken and washed with deionized water to remove the loosely bound ions or impurities. The dye was loaded and pure biomasses were dried at 50˚C for 24 h. The samples were mixed with KBr and then ground in an agate mortar at an approximate ratio for the preparation of pellets. The background obtained from KBr disk was automatically subtracted from the sample discs spectra.

2.8. Analysis

In order to measure the concentration of AB25, 5 mL sample was taken from the reaction mixture and filtered through a 0.2 μm membrane filter (Orange Scientific, GyroDisc CA-PC, Belgium). Then, the absorbance of the supernatant was measured at the wavelength corresponding to the maximum absorbance of the sample. A calibration curve was prepared by measuring absorbance of different concentrations of AB25 solutions at $\lambda_{max} = 600$ nm using a UV/vis Spectrophotometer (Hach, DR/4000 Spectrophotometer, USA).

Mass capacity of adsorption (q_e) was calculated using the mass balance equation given by Eq. (1):

$$q_e = \frac{V(C_i - C_f)}{m} \quad (1)$$

where q_e is the dye sorption (mg/g); C_i and C_f are the initial and equilibrium dyes concentrations in the solution (mg/L), respectively; V is the solution volume (L); and m is the mass of biosorbent (g).

3. Results and discussion

3.1. Effect of initial soloution pH

Literature data showed that during biosorption of dye molecules, the pH of solution played an important role on adsorption capacity of different sorbents [23]. To study the adsorption properties of *P. pusillus* and *C. demersum* biomass, the effect of different initial soloution pH from 2.0 to 10.0 was investigated when the initial concentration of AB25, temperature and biomasses dosage was kept constant. As shown in Fig. 2, removal efficiency (%) of AB25 dye with both aquatic plants decreased with increase in initial

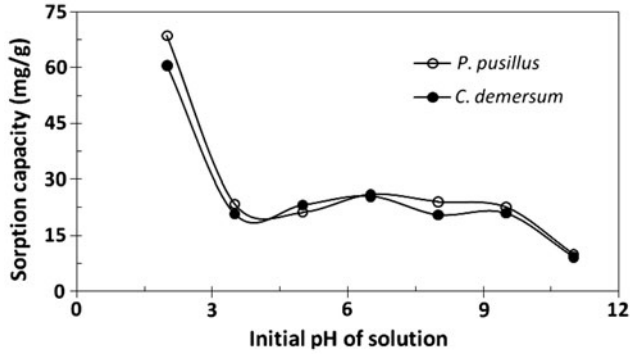

Fig. 2. Effect of initial solution pH on biosorption capacity of AB25 by *P. pusillus* and *C. demersum* biomass, $T = 25 \pm 2$˚C, $[AB25]_o = 30$ mg/L, [Biomass weight] = 0.4 g/L.

solution pH. Accordingly, maximum adsorption of AB25 was obtained at pH of 2 equal to 68.64 mg/g of *P. pusillus* and 60.52 mg/g of *C. demersum*.

The initial solution pH significantly influences the overall adsorption process.

It can influence dissociation of functional groups on the active sites of the biosorbent and the degree of ionization of materials present in the solution [24]. In aqueous solutions, AB25 is first dissolved and its sulfonate groups are dissociated and converted into anionic dye ions. The adsorption process then proceeds due to the electrostatic attractions between the ammonium groups of material and the sulfonate groups of acid dye [25]. On the other hand, aquatic plants have positive surface in acidic aqueous solutions and therefore, the free amino groups are protonated and the biomass becomes fully soluble facilitating electrostatic interaction between sorbents and the negatively charged anionic dyes. This cationic property will influence the adsorption capacity, especially in the case of anionic dyes, depending on the charge and functions of the dye under the corresponding experimental conditions [26]. This result was in agreement with Acid Blue 25 biosorption by raw, esterified and protonated *Jania adhaerens* biomass [27] and biosorption of Acid Blue 25 by the brown macroalga *Stoechospermum marginatum* [1].

3.2. Effect of aquatic plants biomass dosage

The effect of various biomass dosage (0.1–2.5 g/L) on AB25 adsorption was studied while the initial concentration of AB25, temperature, and initial pH of solution were constant at 30 mg/L, 25 ± 2°C and 2, respectively. As can be seen in Fig. 3, the removal percentage of AB25 was significantly increased along with an increase in the amount of biomass. It was found 98.89% for 1 g *P. pusillus*/L and 98.33% for 1.9 g *C. demersum*/L, although removal percentage remind constant at higher biosorbents dosage.

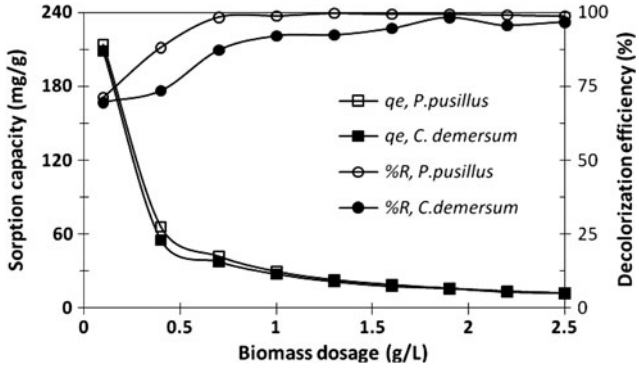

Fig. 3. Effect of different biomass dosages on biosorption capacity of AB25 by *P. pusillus* and *C. demersum* biomass, pH 2, $T = 25 \pm 2$°C, $[AB25]_o = 30$ mg/L.

In the presence of constant initial concentration of AB25, increasing the biomass dosage provided greater surface area and availability of more dye binding sites [28], leading to the improvement of AB25 adsorption. However, a consequence of partial aggregation of biomass at higher biomass dosage was the decrease in effective surface area for the adsorption capacity of AB25 ions [29]. A similar observation was previously reported for Acid Black 1 biosorption by *Cystoseira indica* and *Gracilaria persica* biomasses [30].

As can be seen in Fig. 3, the sorption capacity (mg/g) of biosorbents decreased as their dosage increased. The decrease in sorption capacity may be due to particle aggregation in higher biomass, which causes a decrease in total surface area of the biosorbent and an increase in diffusional path length, the removal efficiency of the dye decreased [31]. This result was consistent with the adsorption studies of acidic dye [32], basic dye [33]. The relationship between the sorption capacity (mg/g) and the biomass dosage (g/L) was obtained with a determination coefficient as high as 0.997 and 0.998 for *P. pusillus* (Eq. (2)) and *C. demersum* (Eq. (3)), respectively:

$$q_e = 28.45x^{-0.89} \quad (2)$$

$$q_e = 26.67x^{-0.88} \quad (3)$$

where q_e is sorption capacity (mg/g) and x the biomass dosage (g/L).

3.3. Effect of biosorbent size on adsorption capacity

The influence of particle size distribution of biosorbent on adsorption capacity of AB25 molecules was studied by aquatic plants biomass at different particle sizes of 53–106, 106–250, and 250–500 μm (Fig. 4). Decreasing particle size of biosorbents resulted increasing biosorption capacity from 67.70 to 71.77 mg/g of *P. pusillus* and 51.77 to 70.83 mg/g of *C. demersum*. As can be seen from Fig. 4, the highest adsorption capacity of 71.77 and 70.83 mg/g was observed for *P. pusillus* and *C. demersum*, respectively, at the smallest particle size of biosorbents tested (53–106 μm). The increase in adsorption capacity may be attributed to larger surface area of the smaller particle size of biosorbent and larger number of ion exchanging sites responsible for dyes binding at the same amount of biomass [34]. In a study, the removal of AB25 and DR80 was investigated using various

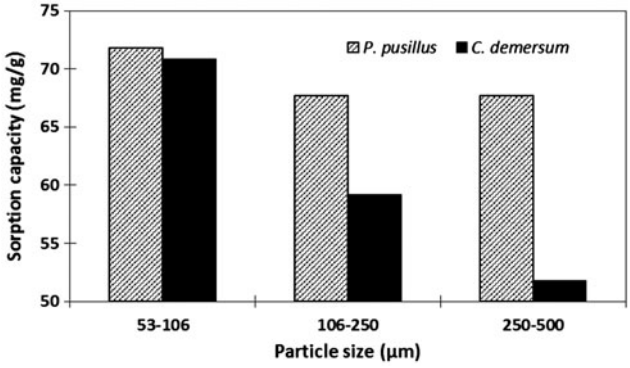

Fig. 4. Effect of different particle sizes of *P. pusillus* and *C. demersum* biomass on biosorption capacity of AB25, pH 2, $T = 25 \pm 2$°C, $[AB25]_o = 30$ mg/L, [Biomass weight] = 0.4 g/L.

ranges of particle sizes from <0.125 to >0.6 μm of egg shell membrane, and maximum adsorption was obtained at the smallest particle size [35]. However, as can be seen from Fig. 4, there is a significant difference in sorption capacity trends of two biosorbents toward particle size. Increasing particle size of biosorbents causes a sharp reduction of sorption capacity for *C. demersum*, while there is no significant reduction for *P. pusillus*. It should be noted that the differences in biosorption capacity between *P. pusillus* and *C. demersum* tested here can be attributed to their structural properties such as protein and carbohydrate composition, surface charge density, topography, and surface area [8].

3.4. Effect of initial dye concentration on adsorption capacity

Fig. 5 shows the effect of initial concentration of AB25 (30–100 mg/L) on the biosorption capacity using

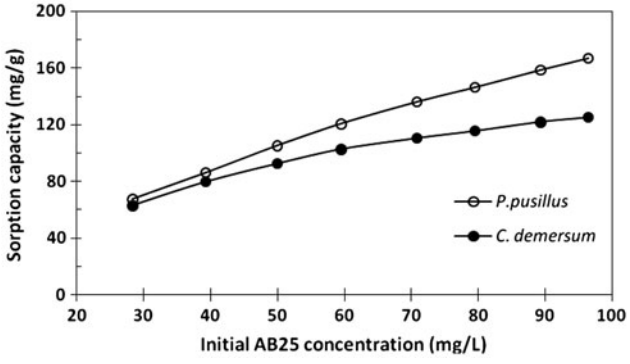

Fig. 5. Effect of initial AB25 concentration on biosorption capacity of AB25 by *P. pusillus* and *C. demersum* biomass, pH 2, $T = 25 \pm 2$°C, [Biomass weight] = 0.4 g/L.

biomasses of *P. pusillus* and *C. demersum*. The biosorption capacity of AB25 was increased from 67.28 to 167.00 mg/g of *P. pusillus* and 62.86 to 125.18 mg/g of *C. demersum* for the initial concentration range of AB25 tested. The reason for this observation can be attributed to the fact that the initial dye concentration provided an important driving force to overcome all mass transfer resistances of the AB25 ions between the aqueous solution and aquatic plants biomass. Furthermore, at higher concentrations, it is not likely that dyes are only adsorbed in a monolayer at the outer interface of biomass. The diffusion of exchanging molecules within biosorbent particles may control the biosorption rate at higher initial concentrations [36]. The result is in agreement with the previously reported in the literature. The initial concentration effect (100–800 mg/L) of Acid Black 172 and Congo Red was investigated from aqueous solution on nonviable *Penicillium* YW01 adsorption capacity. The maximum capacity of dyes sorption was achieved in 800 mg/L initial dye concentration [37].

3.5. Modeling of adsorption isotherms

The results obtained from equilibrium isotherms were analyzed with Langmuir, Freundlich, D–R and Temkin models. The corresponding models constants and the regression correlation coefficients are listed in Table 1. Langmuir model suggests that no strong competition exists between the adsorbate and the solvent to occupy the adsorption sites. The linear Langmuir isotherm is given below [38]:

$$\frac{q_e}{C_e} = bq_{max} - bq_e \quad (4)$$

where q_e (mg/g) and C_e (mg/L) are the amount of dye adsorbed per unit weight of biomass and dye equilibrium concentration in solution at equilibrium, respectively. q_{max} (mg/g) indicates the monolayer sorption capacity of adsorbent and the Langmuir constant b (L/mg) is related to the energy of biosorption.The low values of correlation coefficient for the linearized Langmuir relationships decline the single surface reaction with constant activation energy [24]. The maximum sorption capacity (q_{max}) of AB25 on *P. pusillus* and *C. demersum* obtained from Langmuir model was 183.46 and 129.68 mg/g, respectively. The maximum sorption capacity of AB25 with other sorbents reported in the literature is given in Table 2. The difference in AB25 sorption capacity by various sorbents may be attributed different physicochemical properties of sorbents and experimental conditions [39].

The linear Freundlich isotherm model is shown below [40]:

Table 1
Isotherm constants of AB25 biosorption onto *P. pusillus* and *C. demersum* biomass, pH 2, $T = 25 \pm 2$ °C, $[AB25]_o = 20$–100 mg/L, [Biomass weight] = 0.4 g/L

Biomass	Langmuir model			Freundlich model			D–R model				Temkin model		
	q_m (mg/g)	b (L/mg)	R^2	K_f (mg/g)	n	R^2	q_s(mg/g)	$k_{ad} \times 10^5$ (mol^2/kJ^2)	E (kJ/mol)	R^2	b_T	A_T (L/mg)	R^2
P. pusillus	183.46	0.20	0.91	48.86	2.75	0.99	150.66	0.30	0.41	0.85	61.75	1.91	0.99
C. demersum	129.68	0.25	0.91	47.97	1.79	0.99	117.45	0.40	0.35	0.86	105.11	4.19	0.99

Table 2
Comparison of maximum uptake capacities of Acid Blue 25 by various sorbents

Sorbent	q_m (mg/g)	Source
Stoechospermum marginatum	40.0	[1]
Cationized cellulosic material	288	[58]
Cationic starch	249	[59]
Crosslinked cyclodextrin	88	[60]
Chitosan/cyclodextrin composite	77.4	[61]
Modified silica	45.8	[62]
Egyptian bagasse pith	17.5	[63]
Egyptian bagasse pith	14.4	[45]
Sphagnom moss Peat	12.7	[42]
Diatomite	10.11	[64]
Eichhornia crassipes	9.58	[65]
Calcined diatomite	7.57	[64]
Wood sawdust	5.99	[66]
P. pusillus	183.46	Present work
C. demersum	129.68	Present work

$$\log q_e = \log K_f + 1/n \log C_e \quad (5)$$

where C_e is the sorbate concentration in liquid phase at equilibrium (mg/L), K_f the Freundlich constant ($mg^{1-1/n} L^{1/n} g^{-1}$), and n (dimensionless) an empirical parameter related to the biosorption intensity, which varies according to the heterogeneity of the material.

From non-linear Freundlich isotherm plots, K_f and n values were found to be 48.86 mg/g and 2.75 for *P. pusillus* and 47.97 mg/g and 1.79 for *C. demersum*, respectively. The n values were between 0 and 10 indicating that the adsorption of AB25 using *P. pusillus and C. demersum* biomass was favored at experimental conditions. The R^2 values were found to be 0.99 for both sorbents, indicating that the Freundlich isotherm model was found to provide the best theoretical correlation of the experimental data. Adsorption isotherms of AB25 ions by *P. pusillus* and *C. demersum* are shown in Fig. 6.

The equilibrium data, also subjected to the D–R isotherm model, were used to determine the nature of adsorption processes as physical or chemical. The linear presentation of the D–R isotherm equation [41] is expressed by:

$$\ln q_e = \ln q_m - \beta\varepsilon^2 \quad (6)$$

where q_e is the amount of AB25 adsorbed on per unit weight of biomass (mol/g); q_m is the theoretical adsorption capacity; β is the constant of the sorption energy, which is related to the average energy of

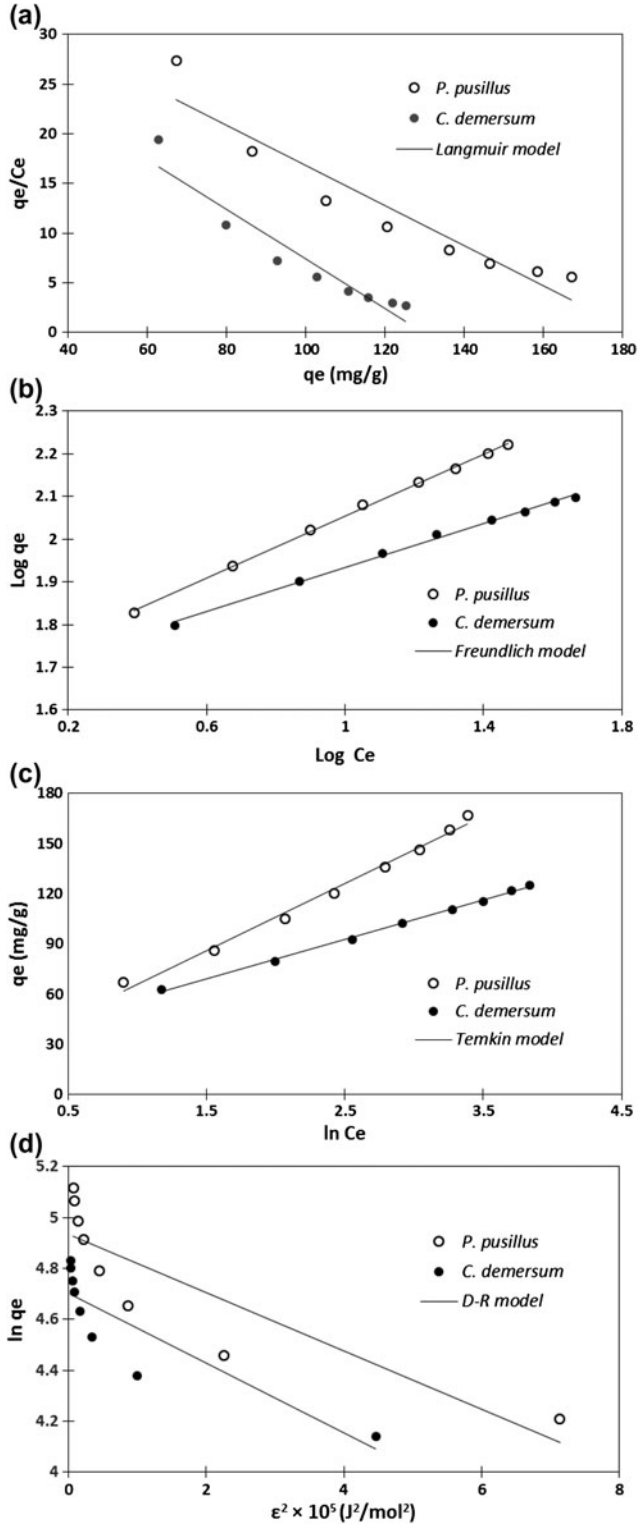

Fig. 6. Biosorption isotherm models of AB25 biosorption by *P. pusillus* and *C. demersum* biomass; Langmuir (a), Freundlich (b), Temkin (c), and D–R (d) models, pH 2, $T = 25 \pm 2$°C, [Biomass weight] = 0.4 g/L.

sorption per mole of the adsorbate as it is transferred to the surface of the solid from infinite distance in the solution; and ε the Polanyi potential ($\varepsilon = RT \ln (1 + 1/C_e)$) – where T is the temperature (K) and R is the gas constant. The value of mean sorption energy, E, can be calculated from D–R parameter b as follows:

$$E = \frac{1}{\sqrt{2\beta}} \tag{7}$$

The E (kJ mol^{-1}) value gives information about biosorption mechanism, and more specifically, its physical or chemical nature. If it lies between 8 and 16 kJ mol^{-1}, the biosorption process is controlled by a chemical mechanism, while for $E < 8$ kJ mol^{-1}, the biosorption process proceeds through a physical mechanism. The mean free energy of adsorption was calculated to be 0.41 and 0.35 kJ/mol for *P. pusillus* and *C. demersum*, respectively. These findings suggest that the adsorption process of AB25 by these biomasses could take place by physical mechanisms.

Another model, Temkin isotherm model, was also used to fit the experimental data. Unlike the Langmuir and Freundlich equations, the Temkin isotherm, taking the interactions between adsorbent-adsorbate in to account, is based on the assumption that the free energy of sorption is a function of the surface coverage [42]. The linear form of isotherm is as follows [43]:

$$q_e = \frac{RT}{b_T} \ln A_T + \left(\frac{RT}{b_T}\right) \ln C_e \tag{8}$$

where A_T, the equilibrium binding constant, corresponds to the maximum binding energy, b_T is the Temkin isotherm constant, T is the temperature (K), and R the ideal gas constant (8.314 J/mol K). The constants of Temkin model listed in Table 1 indicate that the heat of biosorption of dye molecules in the layer decreased linearly with coverage due to adsorbent–adsorbate interactions, and that the adsorption is characterized by a uniform distribution of the binding energies, up to maximum binding energy [43]. These values, confirm that the surface of *Paneous indicus* shell is heterogeneous and possesses equal distribution of binding energies on the available binding sites. The correlation coefficients for both biosorbents were high showing that the experimental data was fitted well to the Temkin isotherm model.

3.6. Effect of contact time

The effect of contact time on biosorption was studied in the time range up to 60 min at initial concentration of 30 mg AB25 /L and 25 ± 2°C using 0.4 g/L

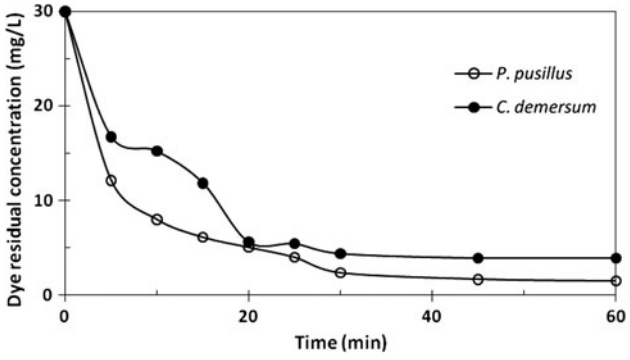

Fig. 7. Effect of contact time on AB25 biosorption onto *P. pusillus* and *C. demersum* biomass, pH 2, $T = 25 \pm 2$°C, $[AB25]_o = 30$ mg/L, [Biomass weight] = 0.4 g/L.

biosorbent of *P. pusillus* and *C. demersum*. As shown in Fig. 7, biosorption was increased rapidly during the first 5 min, followed by a moderate increase up to 20 min; thereafter, the adsorption reached equilibrium up to 60 min. At that time, the amount of dye being adsorbed onto the biomaterial was in a state of dynamic equilibrium with the amount of dye desorbed from the adsorbent [25]. In the adsorption mechanism, at the beginning, the dye molecules are adsorbed externally causing rapid increase of biosorption rate. When the external surface becomes saturated, the dye molecules are absorbed into the porous structure of the biomass [44]. On the other hand, the initial rapid phase may involve physical adsorption or ion exchange at cell surface and the subsequent slower phase may involve other mechanisms such as complexation, microprecipitation or saturation of binding sites. Similar observation was previously reported for the effect of agitation time on the removal of AB25 onto *S. marginatum* [45] and cationized starch-based material [25].

3.7. Kinetic modeling of AB25 biosorption

Kinetic models are used to examine the controlling mechanism of biosorption process such as biosorption surface, chemical reaction and/or diffusion mechanism. In order to determine the adsorption kinetics of AB25 by *P. pusillus* and *C. demersum* biomass, three kinetic models including Lagergren's pseudo-first-order model, pseudo-second-order model, and intraparticle diffusion model were applied to the experimental data. The applicability of these kinetic models was determined by measuring the coefficients of determination (R^2), as shown in Table 3. The linear form of the pseudo-first-order rate equation is given as [46]:

Table 3
Kinetic parameters obtained from pseudo-first-order model, pseudo-second-order model, and intraparticle diffusion of AB25 biosorption onto *P. pusillus* and *C. demersum* biomass, pH 2, $T = 25 \pm 2$°C, $[AB25]_o = 30$ mg/L, [Biomass weight] = 0.4 g/L

Biomass	Pseudo-first-order			Pseudo-second-order			Intraparticle diffusion		
	$k_{1\times10}$ (1/min)	q_1 (mg/g)	R^2	$k_{2\times10^2}$ (g/mg min)	q_2 (mg/g)	R^2	$k_{id\times10}$ (mg g min$^{-0.5}$)	C	R^2
P. pusillus	1.03	54.05	0.97	0.43	125.00	0.99	4.66	89.67	0.87
C. demersum	1.77	167.50	0.95	0.28	125.00	0.99	6.51	77.53	0.78

$$\frac{1}{q_t} = \frac{k_1}{q_1 t} + \frac{1}{q_1} \tag{9}$$

where q_t is the amount of adsorbate at time t (mg g^{-1}), q_1 is the biosorption capacity in equilibrium (mg g^{-1}), k_1 is the rate constant of the equation (min^{-1}), and t is time (min). The coefficients of determination of 0.95 for *P. pusillus* and 0.97 for *C. demersum* at the temperature studied are low (Table 3). The pseudo-first-order model is not useful for modeling the biosorption of AB25 in this work and there is a significant difference between calculated and experimental values.

Experimental data were also evaluated by the pseudo-second-order kinetic model, which is given in the following form [42]:

$$\frac{t}{q_t} = \frac{1}{k_2 q_2^2} + \frac{t}{q_2} \tag{10}$$

where q_e and q_2 have the same meaning as mentioned previously, and k_2 (g mg^{-1} min^{-1}) is the rate constant for the pseudo-second-order kinetics. The rate constant, the R^2 and q_2 values are given in Table 3. The R^2 values were 0.99 for both biosorbents suggesting that the present biosorption system can be defined more favorably by the pseudo-second-order kinetic model (Fig. 8).

The results also show that the biosorption of dye probably took place through surface exchange reactions until the surface functional sites were fully occupied; thereafter, dye molecules diffuse into the sorbent network for further interactions. The dye diffusion within the particle is much slower than its movement from solution to the external solid surface because of the greater mechanical obstruction to movement presented by the surface molecules or surface layers and the restraining chemical attractions between dye and adsorbent [47].

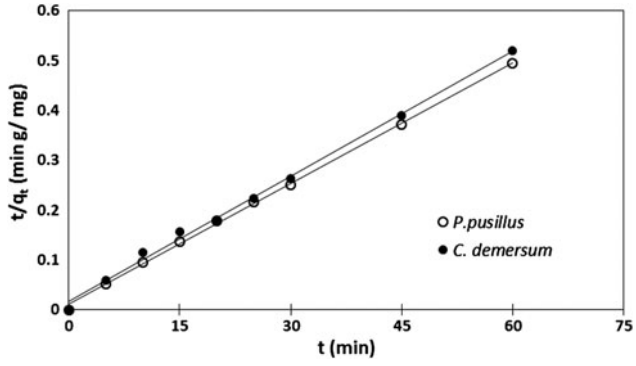

Fig. 8. Pseudo-second-order kinetic model plot for the biosorption of AB25 onto *P. pusillus* and *C. demersum* biomass, pH 2, $T = 25 \pm 2$°C, $[AB25]_o = 30$ mg/L, [Biomass weight] = 0.4 g/L.

The Webber–Morris plots (1963) gave three-stage sections, which mean an instantaneous adsorption stage, a gradual adsorption stage, and final equilibrium stage in sequence.

The intra-particle diffusion model is expressed as follows [4]:

$$q = k_{id} t^{0.5} + c \tag{11}$$

where q (mg/g) is the amount of AB25 adsorbed at time t, c is the intercept, and k_{id} (mg/g min$^{0.5}$) is the intraparticle diffusion rate constant. As shown in Fig. 8, the linear plot of intra-particle diffusion model between the AB25 and biomasses did not pass through the origin. This deviation from the origin may be due to the difference in the rate of mass transfer in the initial and final stages of adsorption [48]. This, being indicative of some degree of boundary layer control, showed that the intra-particle diffusion was not the rate-limiting step of adsorption process of AB25 on biosorbents tested at experiment temperature.

Therefore, based on the correlation coefficient values in Table 3, it can be inferred that adsorption of AB25 onto biomass followed pseudo-second-order model. According to the results, there is a rate-limiting step in biosorption mechanism and mass transfer was not involved in solution [49].

3.8. Thermodynamic study of AB25 adsorption

In order to investigate thermodynamic behavior of the biosorption of AB25 onto *P. pusillus* and *C. demersum* biomass, thermodynamic parameters including the changes in free energy (ΔG°), enthalpy (ΔH°) and entropy (ΔS°) were calculated from the following equations [19]:

$$\Delta G^\circ = -RT \ln K_D \tag{12}$$

$$\ln K_D = \frac{\Delta S^\circ}{R} - \frac{\Delta H^\circ}{RT} \tag{13}$$

where R is the universal gas constant (8.314 J/mol.K), T is the temperature (K), and K_D (q_e/C_e) is the distribution coefficient. Gibbs free energy change (ΔG°) was calculated to be −4.77, −5.67 and −6.80 kJ/mol for *P. pusillus* and −3.19, −3.66 and −4.26 for *C. demersum* at 10, 25 and 40°C, respectively (Table 4). The negative (ΔG°) values indicated thermodynamically feasible and spontaneous nature of the biosorption.

Table 4
Thermodynamic constants of AB25 biosorption onto *P. pusillus* and *C. demersum* biomass, pH 2, $[AB25]_o = 30\,mg/L$, [Biomass weight] = 0.4 g/L

Biomass	ΔH° (kJ/mol)	ΔS° (J/mol K)	ΔG° (kJ/mol)			R^2
			10 °C	25 °C	40 °C	
P. pusillus	14.37	67.54	−4.77	−5.67	−6.80	0.990
C. demersum	6.88	35.52	−3.19	−3.66	−4.26	0.988

The increase in negative (ΔG°) values by temperature shows an increase in feasibility of biosorption at higher temperatures. This is because higher temperatures provide faster rates of diffusion of adsorbate molecules from the solution to the biosorbent. Also, the solubility of the dye increases and then, the interaction forces become stronger between the solute and the solvent [50]. (ΔH°)and (ΔS°) values were found to be 14.37 kJ/mol and 67.54 J/mol K for *P. pusillus* and 6.88 kJ/mol and 35.52 J/mol K for *C. demersum* at all temperatures tested. The positive (ΔH°) indicates the endothermic nature of the adsorption processes at 15–40 °C. Furthermore, the positive value of (ΔS°) reveals the increased randomness at the solid–solution interface during the fixation of the AB25 on the binding sites of the biomasses surface.

3.9. Effect of neutral salts and salinity

Textile wastewaters contain various acids, alkalis, salts, metal ions and other impurities. The presence of such ions affects the dye biosorption capacity of biosorbents [51]. Fig. 9(a) demonstrates the effects of

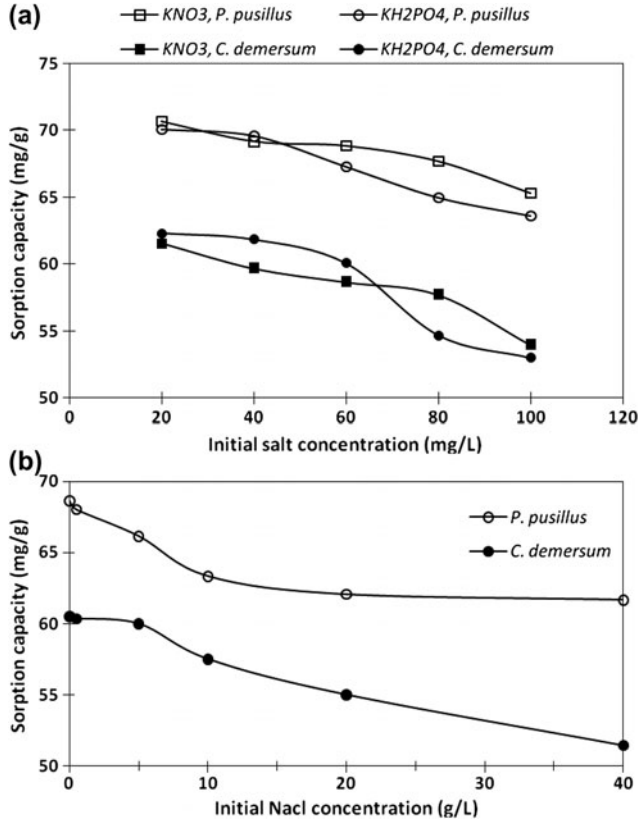

Fig. 9. Effects of neutral salts (a) and salinity (b) on biosorption capacity of AB25 onto *P. pusillus* and *C. demersum* biomass, pH 2, $T = 25 \pm 2$ °C, $[AB25]_o = 30\,mg/L$, [Biomass weight] = 0.4 g/L.

nitrate and phosphate salts as neutral salts on AB25 adsorption capacity of *P. pusillus* and *C. demersum* in aqueous solutions. The results show that the dye biosorption capacity onto *P. pusillus* decreased from 70.73 to 65.31 mg/g and from 70.10 to 61.64 mg/g in the presence of 20–100 mg/L nitrate and phosphate salt, respectively. The dye biosorption capacity onto *C. demersum* decreased from 61.56 to 53.95 mg/g and from 62.29 to 53.02 mg/g in the concentration range of 20–100 mg/L nitrate and phosphate salt, respectively. The increased amount of electrolyte can occupy the sorbent surface, decreasing dye ion available to the biomass surface for sorption and therefore, the dye biosorption capacity may be significantly decreased [52]. Also, the observed decrease in the sorption of AB25 could be explained by considering the competitive effect of nitrate and phosphate anions on dye binding sites of biosorbents. In addition, the cations such as K^+ are expected to form complexes with anionic division (sulfonate groups) of dye.

Sodium chloride is often used as a stimulator in dyeing processes. Therefore, the effect of different NaCl concentrations, from deionized water to hypersaline water, on dye biosorption was studied by aquatic plants *P. pusillus* and *C. demersum*, as shown in Fig. 9(b). As can be seen from this figure, the biosorption capacity was decreased from 68.84 to 61.67 mg/g for *P. pusillus* and 60.52–51.46 mg/g for *C. demersum* along with an increase in salt concentration from 0 to 40 g/L in dye solutions. The results showed that dye biosorption decreased with an increase in water salinity. The effects of ion strength on sorption of Basic Blue 9 and phosphoric acid modified rice straw were tested by the addition of sodium chloride (ranged from 0 to 0.5 M) to the dye solutions. Increasing the ion strength of solution caused a sharp decrease in sorption percentages of Basic Blue 9 [53]. In another investigation, the addition of NaCl (250 mg/L) to the dye solution caused only a 2% decrease in decolorization efficiency of Acid Yellow 23 [54]. NaCl salt may screen the electrostatic interaction of opposite charges in adsorbents surface and the dye molecules, and an increase in salt concentration could decrease the amount of dye adsorbed [24].

3.10. FT-IR analysis of adsorbent–adsorbate interaction

The FT-IR method was conducted to obtain information on the nature of possible interactions between the functional groups of biomass and AB25 ions. The FT-IR spectra of biomass before and after dye treatment are shown in Fig. 10(a)–(d).

The broad and strong vibration around 3,000–3,600 cm^{-1} is indicative of the presence of the -OH groups and -NH groups on biosorbent biomasses. The peaks at 2,840–2,990 cm^{-1} are assigned the asymmetric and symmetric C–H stretching of the aliphatic groups. The strong peaks at 1637.27 cm^{-1} and 1638.23 cm^{-1} for *P. pusillus* and *C. demersum* biomass, respectively, were attributed to stretching vibration of carboxyl group (–C=O). The peaks at 1449.24 and 1458.89 cm^{-1} represent -N-H bending vibration for *P. pusillus* and *C. demersum*, respectively. The peak at 1384.64 is due to –N=O stretching vibrations for the biomasses. The bands observed at 1,015–1,273 cm^{-1} were assigned to C–O stretching vibration of alcohols and carboxylic acids. Therefore, these bands (Figs. 10(a) and (c)) confirm the lignin structure of the biomasses [55,56].

Comparison of dye-loaded biomass with FTIR spectra of pure biomass displayed significant changes in some of the peaks. As can be seen in Fig. 10(b), the shift and sharp reduction of the 3422.06 cm^{-1} peak to 3420.14 cm^{-1} suggests the major role of–OH and –NH group for AB25 biosorption onto *P. pusillus* biomass. There was a clear disappearance of the bands 2854.13 and 1734.66 cm^{-1} after dye was loaded onto biomass. The significant reduction in the peak at 1637.27 cm^{-1} reflects the effect of carboxyl group upon binding of AB25 ions. The peaks were shifted in the bands 1449.24–1424.17 cm^{-1} and 1104.05–1097.3 cm^{-1} after dye treatment. In the *C. demersum* biomass, the great shift and reduction of the 3419.17 cm^{-1} peak to 3433.64 cm^{-1} indicate that the hydroxyl and amine groups are the most important functional groups for biosorption of AB25 dye. Two peaks were added in the bands 1725.1 and 1534.1 cm^{-1} after treatment, which was taken as a sign of biomass enrichment. The peaks shift and reduction at 1638.23–1628.59 cm^{-1} and 1114.65–1076.08 cm^{-1} may be due to the involvement of these functional groups in the biosorption process (Fig. 10(d)). Also, the peaks in the region of lower wave numbers (under 1,000 cm^{-1}) appeared as a broad peak and this may be attributed to an interaction between dye ions and N-containing chemical ligands of biomass [57].

These observations indicate that several functional groups on the surface of the biomasses are responsible for binding of AB25 ions in the adsorption process. Moreover, different adsorption capacities of AB25 onto *P. pusillus* and *C. demersum* biomass may be attributed to the different interactions between dye molecule and the biomasses.

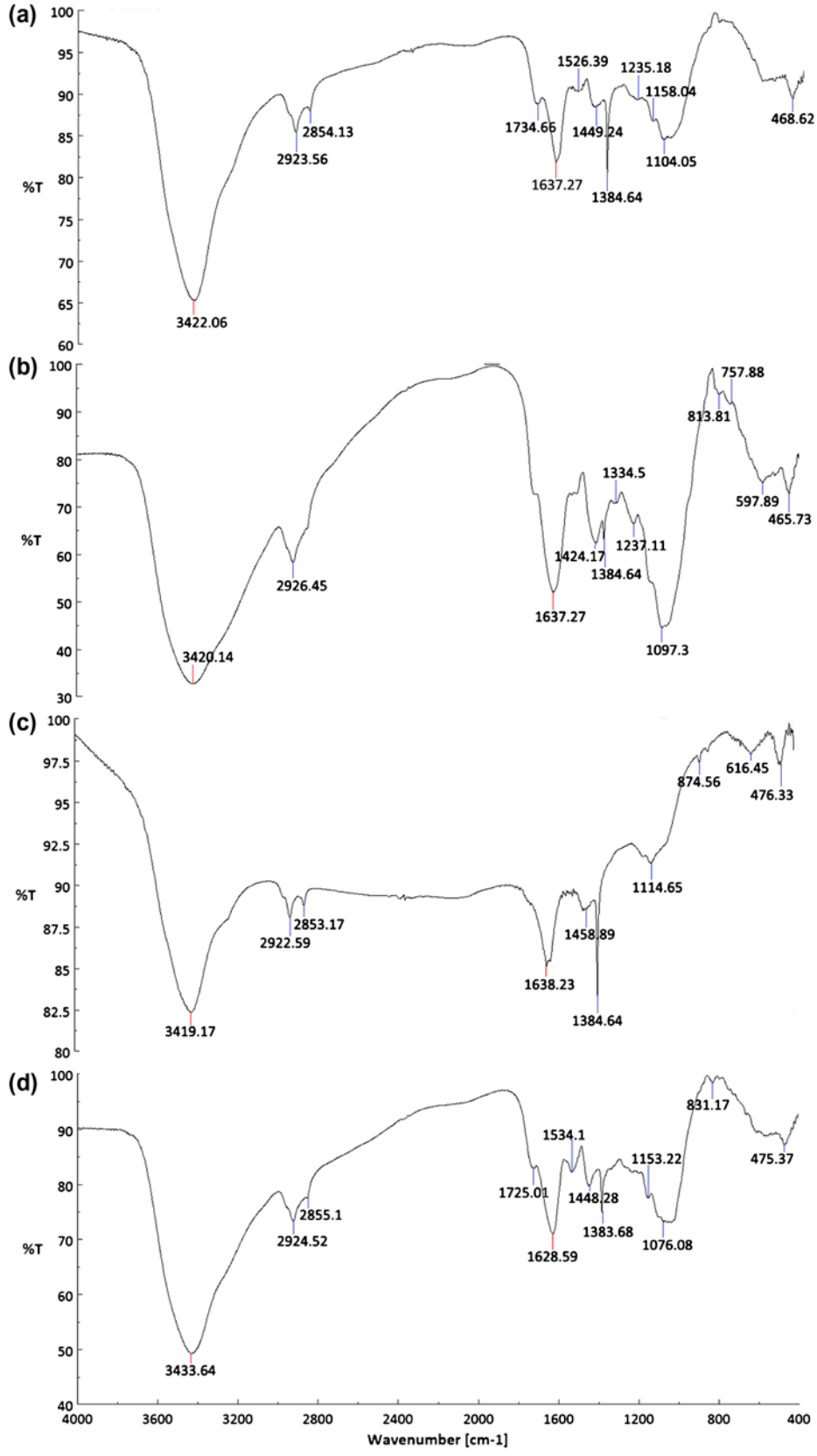

Fig. 10. FT−IR spectra of AB25 biosorption onto *P. pusillus* before (a), after (b), and *C. demersum* before (c), after (d) treatment. pH 2, $T = 25 \pm 2$ ℃, $[AB25]_o = 30$ mg/L, [Biomass weight] = 0.4 g/L.

4. Conclusion

The results of this study demonstrated that the aquatic plants *P. pusillus* and *C. demersum* biomasses were efficient as biosorbents for the sorption of AB25 from wastewater effluents. The biosorption process depends significantly on the pH of the solution and is favored at pH 2.0. Biosorption of AB25 onto aquatic plants could be well described by the pseudo-second-order kinetic model. The biosorption process follows Freundlich and Temkin isotherm model. Physical biosorption in the biomasses and chemical interaction of the dye molecules were both involved in the biosorption process. Negative Gibbs free energy has been evaluated with the change in temperature (15–40˚C) indicating a spontaneous and endothermic process. The study implied that *P. pusillus and C. demersum* can be considered as suitable biomaterials for removal of dyes from textile wastewater.

Acknowledgments

The authors are grateful for the financial support by Student Affairs of Isfahan University of Technology, Isfahan Water and Sewage Company and Isfahan Municipality. The authors also would like to thank Isfahan University of Technology students, Negin Koutahzadeh and Mohammad Salar Sohrabi, for their help in laboratory. Also we would like to thank Hossein Mortazavi and Adib Jaberi, the staffs of Isfahan Water and Sewage Company, for providing laboratory facilities.

References

[1] E. Daneshvar, M. Kousha, M.S. Sohrabi, A. Khataee, A. Converti, Biosorption of three acid dyes by the brown macroalga *Stoechospermum marginatum*: Isotherm, kinetic and thermodynamic studies, Chem. Eng. J. 195–196 (2012) 297–306.

[2] M. Kousha, E. Daneshvar, M.S. Sohrabi, M. Jokar, A. Bhatnagar, Adsorption of acid orange II dye by raw and chemically modified brown macroalga *Stoechospermum marginatum*, Chem. Eng. J. 192 (2012) 67–76.

[3] R. Cheng, Z. Jiang, S. Ou, Y. Li, B. Xiang, Investigation of Acid Black 1 adsorption onto amino-polysaccharides, Polym. Bull. 62 (2009) 69–77.

[4] W.J. Weber, J.C. Morris, Kinetics of adsorption on carbon from solution, J. Sanit. Eng. Div. 89 (1963) 31–59.

[5] I. Bouzaid, C. Ferronato, J.M. Chovelon, M.E. Rammah, H. J.M, Heterogeneous photocatalytic degradation of the anthraquinonic dye, Acid Blue 25 (AB25): A kinetic approach, J, Photochem. Photobiol. 168 (2004) 23–30.

[6] A.R. Khataee, V. Vatanpour, A.R. Amani Ghadim, Decolorization of C.I. Acid Blue 9 solution by UV/Nano-TiO2, Fenton, Fenton-like, electro-Fenton and electrocoagulation processes: A comparative study, J. Hazard. Mater. 161 (2009) 1225–1233.

[7] A. Aleboyeh, M.B. Kasiri, M.E. Olya, H. Aleboyeh, Prediction of azo dye decolorization by UV/H2O2 using artificial neural networks, Dyes Pigments 77 (2008) 288–294.

[8] N. Daneshvar, D. Salari, A.R. Khataee, Photocatalytic degradation of azo dye acid red 14 in water on ZnO as an alternative catalyst to TiO_2, J. Photochem. Photobiol. Chem. 162 (2004) 317–322.

[9] T. Ramachandra, N. Ahalya, R. Kanamadi, Biosorption: Techniques mechanisms, CES Technical Report 110, Centre for Ecological Sciences, Indian Institute of Science, Bangalore, 2005.

[10] I. Haq, H.N. Bhatti, M. Asgher, Removal of solar red BA textile dye from aqueous solution by low cost barley husk: Equilibrium, kinetic and thermodynamic study, Can. J. Chem. Eng. 89 (2011) 593–600.

[11] H.N. Bhatti, Y. Safa, Removal of anionic dyes by rice milling waste from synthetic effluents: Equilibrium and thermodynamic studies, Desalin. Water Treat. 48 (2012) 267–277.

[12] A. Mittal, V. Thakur, V. Gajbe, Adsorptive removal of toxic azo dye Amido Black 10B by hen feather, Environ. Sci. Pollut. Res. 20 (2013) 260–269.

[13] A. Mittal, V. Thakur, J. Mittal, H. Vardhan, Process development for the removal of hazardous anionic azo dye Congo red from wastewater by using hen feather as potential adsorbent, Desalin. Water Treat. 51 (2013) 1–11.

[14] A. Mittal, V. Thakur, V. Gajbe, Evaluation of adsorption characteristics of an anionic azo dye Brilliant yellow onto hen feathers in aqueous solutions, Environ. Sci. Pollut. Res. 19 (2012) 2438–2447.

[15] Y. Safa, H.N. Bhatti, Kinetic and thermodynamic modeling for the removal of Direct Red-31 and Direct Orange-26 dyes from aqueous solutions by rice husk, Desalination 272 (2011) 313–322.

[16] S.W. Won, S.B. Choi, Y.S. Yun, Interaction between protonated waste biomass of *Corynebacterium glutamicum* and anionic dye Reactive Red 4, Colloids Surf. A. 262 (2005) 175–280.

[17] T.S. Trung, C.H. Ng, W.F. Stevens, Characterization of decrystallized chitosan and its application in biosorption of textile dyes, Biotechnol. Lett. 25 (2005) 1185–1190.

[18] N. Dhaneshvar, M. Ayazloo, A.R. Khataee, M. Pourhassan, Biological decolorization of dye solution containing Malachite Green by microalgae *Cosmarium* sp, Bioresour. Technol. 98 (2007) 1176–1182.

[19] R. Aravindhan, J.R. Rao, B.U. Nair, Removal of basic yellow dye from aqueous solution by sorption on green alga *Caulerpa scalpelliformis*, J. Hazard. Mater. 142 (2007) 68–76.

[20] K.S. Low, C.K. Lee, L.L. Heng, Sorption of basic dyes by *Hydrilla verticillata*, Environ. Technol. 14 (1993) 115–124.

[21] K.S. Low, C.K. Lee, K.K. Tan, Biosorption of basic dye by water hyacinth roots, Bioresour. Technol. 52 (1995) 79–83.

[22] J.K. Cronk, M.S. Fennessy, Wetland Plants: Biology and Ecology, CRC Press/Lewis, Boca Raton, FL, 2001.

[23] Z. Aksu, I.A. Isoglu, Use of dried sugar beet pulp for binary biosorption of Gemazol Turquoise Blue G reactive dye and copper(II) ions—Equlibrium modeling, Chem. Eng. J. 127 (2007) 177–188.

[24] G. Crini, P.-M. Badot, Application of chitosan, a natural aminopolysaccharide, for dye removal from aqueous solutions by adsorption processes using batch studies: A review of recent literature, Prog. Polym. Sci. 33 (2008) 399–447.

[25] F. Renault, N. Morin-Crini, F. Gimbert, P. Badot, G. Crini, Cationized starch-based material as a new ion-exchanger adsorbent for the removal of C.I. Acid Blue 25 from aqueous solutions, Bioresour. Technol. 99 (2008) 7573–7586.

[26] E. Guibal, P. McCarrick, J.M. Tobin, Comparison of the adsorption of anionic dyes on activated carbon and chitosan derivatives from dilute solutions, Sep. Sci. Technol. 38 (2003) 3049–3073.

[27] M. Kousha, E. Daneshvar, A.R. Esmaeli, M. Jokar, A.R. Khataee, Optimization of Acid Blue 25 removal from aqueous solutions by raw, esterified and protonated *Jania adhaerens* biomass, Int. Biodeterior. Biodegrad. 69 (2012) 97–105.

[28] Y.S. Ho, D.A. John Wase, C.F. Forster, Batch nickel removal from aqueous solution by sphagnum moss peat, Water Res. 29 (1995) 1327–1332.
[29] S. Karthikeyan, R. Balasubramanian, C.S.P. Iyer, Evaluation of the marine algae *Ulva fasciata* and *Sargassum* sp. for the adsorption of Cu(II) from aqueous solutions, Bioresour. Technol. 98 (2007) 452–455.
[30] M. Kousha, E. Daneshvar, M.S. Sohrabi, N. Koutahzadeh, A. R. Khataee, Optimization of C.I. Acid black 1 biosorption by *Cystoseira indica* and *Gracilaria persica* biomasses from aqueous solutions, Int. Biodeterior. Biodegrad. 67 (2012) 56–63.
[31] S.R. Shukla, R.S. Pai, Adsorption of Cu(II), Ni(II) and Zn(II) on dye loaded groundnut shells and sawdust, Sep. Purif. Technol. 43 (2005) 1–8.
[32] A. Ozer, G. Akkaya, M. Turabik, Biosorption of Acid Red 274 (AR 274) on *Enteromorpha prolifera* in a batch system, J. Hazard. Mater. 126 (2005) 119–127.
[33] W.-T. Tsai, H.-R. Chen, Removal of malachite green from aqueous solution using low-cost chlorella-based biomass, J. Hazard. Mater. 175 (2010) 844–849.
[34] H.C. Chu, K.M. Chen, Reuse of activated sludge biomass: I. Removal of basic dyes from wastewater by biomass, Process Biochem. 37 (2002) 595–600.
[35] M. Arami, N.Y. Limaee, N.M. Mahmoodi, Investigation on the adsorption capability of egg shell membrane towards model textile dyes, Chemosphere 65 (2006) 1999–2008.
[36] M.S. Chiou, P.Y. Ho, H.Y. Li, Adsorption of anionic dye in acid solutions using chemically cross-linked chitosan beads, Dyes Pigm. 60 (2004) 69–84.
[37] Y. Yang, G. Wang, B. Wang, Z. Li, X. Jia, Q. Zhou, Y. Zhao, Biosorption of Acid Black 172 and Congo Red from aqueous solution by nonviable Penicillium YW 01: Kinetic study, equilibrium isotherm and artificial neural network modeling, Bioresour. Technol. 102 (2011) 828–834.
[38] I. Langmuir, The adsorption of gases on plane surfaces of glass. Mica and Platinium, J. Am. Chem. Soc. 40 (1918) 1361–1403.
[39] M. Amini, H. Younesi, Biosorption of Cd(II), Ni(II) and Pb(II) from aqueous solution by dried biomass of *Aspergillus niger*: Application of response surface methodology to the optimization of process parameters, Clean 37 (2009) 776–786.
[40] H.M.F. Freundlich, Uber die adsorption in losungen [Over the adsorption in the solution], J. Phys. Chem. 57 (1906) 385–470.
[41] M.M. Dubinin, E.D. Zaverina, L.V. Radushkevich, Sorption and structure of active carbons. I. Adsorption of organic vapors, Zh. Fiz. Khim. 21 (1947) 1351–1362.
[42] Y.S. Ho, G. McKay, Sorption of dye from aqueous solution by peat, Chem. Eng. J. 70 (1998) 115–124.
[43] M.I. Temkin, V. Pyzhev, Kinetics of ammonia synthesis on promoted iron catalysts, Acta Physiochim. 12 (1940) 327–356.
[44] F. Colak, N. Atar, A. Olgun, Biosorption of acidic dyes from aqueous solution by *Paenibacillus macerans*: Kinetic, thermodynamic and equilibrium studies, Chem. Eng. J. 150 (2009) 122–130.
[45] Y.S. Ho, G. McKay, Sorption of dyes and copper ions onto biosorbents, Process Biochem. 38 (2003) 1047–1061.
[46] S. Lagergren, Zur theorie der sogenannten adsorption geloster stoffe [About the theory of so-called adsorption of soluble substances], K. Sven. Vetenskapsakad. Handl. 24 (1898) 1–39.
[47] G. McKay, H.S. Blair, J.R. Gardner, I.F. McConvey, Two resistance mass transport model for the adsorption of various dyestuffs onto chitin, J. App. Polym. Sci. 30 (1985) 4325–4335.
[48] D.H.K. Reddy, K.A. Seshaiah, V.R. Reddy, M.M. Rao, M.C. Wang, Biosorption of Pb^{2+} from aqueous solutions by *Moringa oleifera* bark: Equilibrium and kinetic studies, J. Hazard. Mater. 174 (2010) 831–838.
[49] F.C. Wu, R.L. Tseng, R.S. Juang, Kinetic modeling of liquid-phase adsorption of reactive dyes and metal ions on chitosan, Water Res. 35 (2001) 613–618.
[50] K.G. Bhattacharyya, S.S. Gupta, Removal of Cu(II) by natural and acid-activated clays: An insight of adsorption isotherm, kinetic and thermodynamics, Desalination 272 (2011) 66–75.
[51] P. Kaushik, A. Malik, Fungal dye decolorization: Recent advances and future potential, Environ. Int. 37 (2009) 127–141.
[52] A. Rathinam, B. Maharshi, S.K. Janardhanan, R.R. Jonnalagadda, B.U. Nair, Biosorption of cadmium metal ion from simulated wastewaters using *Hypnea valentiae* biomass: A kinetic and thermodynamic study, Bioresour. Technol. 101 (2010) 1466–1470.
[53] R. Gong, Y. Jin, J. Chen, Y. Hu, J. Sun, Removal of basic dyes from aqueous solution by sorption on phosphoric acid modified rice straw, Dyes Pigm. 73 (2007) 332–337.
[54] N. Modirshahla, M.A. Behnajady, F. Ghanbary, Decolorization and mineralization of C.I. Acid Yellow 23 by Fenton and photo-Fenton processes, Dyes Pigm. 73 (2007) 305–310.
[55] R. Nadeem, T.M. Ansari, A.M. Khalid, Fourier transform Infrared spectroscopic characterization and optimization of Pb(II) biosorption by fish (*Labeo rohita*) scales, J. Hazard. Mater. 156 (2008) 64–73.
[56] A. Selatnia, A. Boukazoula, N. Kechid, M.Z. Bakhti, A. Chergui, Biosorption of Fe^{3+} from aqueous solution by a bacterial dead *Streptomyces rimosus* biomass, Process Biochem. 39 (2004) 1643–1651.
[57] T. Akar, S. Tunali, Biosorption performance of *Botrytis cinerea* fungal byproducts for removal of Cd(II) and Cu(II) ions from aqueous solutions, Miner. Eng. 18 (2005) 1099–1109.
[58] M.H.V. Baouab, R. Gauthier, H. Gauthier, B. Chabert, M.E.B. Rammah, Immobilization of residual dyes onto ion-exchanger cellulosic materials, J. App. Polym. Sci. 77 (2000) 171–183.
[59] F. Delval, G. Crini, N. Morin, J. Vebrel, S. Bertini, G. Torri, The sorption of several types of dye on crosslinked polysaccharides derivatives, Dyes Pigm. 53 (2002) 79–92.
[60] G. Crini, Studies of adsorption of dyes on beta-cyclodextrin polymer, Bioresour. Technol. 90 (2003) 193–198.
[61] B. Martel, M. Devassine, G. Crini, M. Weltrowski, M. Bourdonneau, M. Morcellet, Preparation and sorption properties of a betacyclodextrin-linked chitosan derivative, J. Polym. Sci. 39 (2001) 169–176.
[62] T.N.T. Phan, M. Bacquet, M. Morcellet, Synthesis and characterization of silica gels functionalized with monochlorotriazinyl betacyclodextrin and their sorption capacities towards organic compounds, J. Inclusion Phenom. Macrocyclic Chem. 38 (2000) 345–359.
[63] B. Chen, C.W. Hui, G. McKay, Film-pore diffusion modelling and contact time optimisation for the adsorption of dyestuffs on pith, Chem. Eng. J. 84 (2001) 77–94.
[64] K. Badii, F.D. Ardejani, M.A. Saberi, N.Y. Limaee, S.Z. Shafaei, Adsorption of Acid Blue 25 dye on diatomite in aqueous solutions, Indian J. Chem. Technol. 17 (2010) 7–16.
[65] M.M. El Zawahry, M.M. Kamel, Removal of azo and anthraquinone dyes from aqueous solutions by *Eichhornia Crassipes*, Water Res. 38 (2004) 2967–2972.
[66] Y.S. Ho, G. McKay, Kinetic models for the sorption of dye from aqueous solution by wood, Trans. Inst. Chem. Eng. 76 (1998) 183–191.